Published in final edited form as:
Acta Biomater. 2011 January ; 7(1): 144–151. doi:10.1016/j.actbio.2010.07.020.

Ingrowth of Human Mesenchymal Stem Cells into Porous Silk Particle Reinforced Silk Composite Scaffolds: An *In Vitro* Study

Danielle N. Rockwood[a], **Eun Seok Gil**[a], **Sang-Hyug Park**[a], **Jonathan A. Kluge**[a], **Warren Grayson**[b], **Sarindr Bhumiratana**[b], **Rangam Rajkhowa**[c], **Xungai Wang**[c], **Sung Jun Kim**[d], **Gordana Vunjak-Novakovic**[b], and **David L Kaplan**[a,*]

[a] Department of Biomedical Engineering, Tufts University, Medford, MA, USA

[b] Department of Biomedical Engineering, Columbia University, New York, NY, USA

[c] Centre for Material and Fibre Innovation, Deakin University, Geelong, Victoria, Australia

[d] Department of Pathology, East-West Neo Medical Center, Kyung Hee University, Seoul, Korea

Abstract

Silk fibroin protein is biodegradable and biocompatible, exhibiting excellent mechanical properties for various biomedical applications. However, porous 3D silk fibroin scaffolds, or silk sponges, usually fall short in matching the initial mechanical requirements for bone tissue engineering. In the present study, silk sponge matrices were reinforced with silk microparticles to generate protein-protein composite scaffolds with desirable mechanical properties for *in vitro* osteogenic tissue formation. It was found that increasing the silk microparticle loading led to a substantial increase in the scaffold compressive modulus from 0.3 MPa (nonreinforced) to 1.9 MPa for 1:2 (matrix:particle) reinforcement loading by dry mass. Biochemical, gene expression, and histological assays were employed to study the possible effects of increasing composite scaffold stiffness, due to microparticle reinforcement, on *in vitro* osteogenic differentiation of human mesenchymal stem cells (hMSCs). Increasing silk microparticle loading increased the osteogenic capability of hMSCs in the presence of bone morphogenic protein-2 (BMP-2) and other osteogenic factors in static culture for up to six weeks. The calcium adsorption increased dramatically with increasing loading, as observed from biochemical assays, histological staining, and microCT (μCT) analysis. Specifically, calcium content in the scaffolds increased by 0.57, 0.71, and 1.27 mg (per μg of DNA) from 3 to 6 weeks for matrix to particle dry mass loading ratios of 1:0, 1:1 and 1:2, respectively. In addition, μCT imaging revealed that at 6 weeks, bone volume fraction increased from 0.78% for nonreinforced to 7.1% and 6.7% for 1:1 and 1:2 loading, respectively. Our results support the hypothesis that scaffold stiffness may strongly influence the 3D *in vitro* differentiation capabilities of hMSCs, providing a means to improve osteogenic outcomes.

Keywords

osteogenesis; human mesenchymal stem cells (hMSCs); silk; composite; matrix stiffness

[*]Corresponding author Tel.: +1 (617) 627 3251 Fax: +1 (617) 627 3231. david.kaplan@tufts.edu (D.L. Kaplan) Postal Address: 4 Colby Street, Medford, MA 02155.

1 Introduction

Large bony defects, from either non-unions or trauma, can pose a significant problem for a patient and often require surgical intervention [1]. Current treatments rely on autografts or allografts, each of which has associated risks. Autografts require an additional surgical site, with a restricted amount of available donor tissue, and are often associated with donor site morbidity. In contrast, the issue of limited donor material is alleviated with the use of allografts, although there is a potential risk of disease transmission and possible long-term complications [2,3]. In some cases, it has been shown that progenitor cells can be injected into the defect to aid in tissue repair [4]. Although this approach has shown some promise, difficulty remains with immobilizing the cells at the site of bone regeneration. Therefore, tissue engineered constructs have been considered in order to sustain cells at the implant site and furthermore to act as conduits for growth factor, antibiotic, or therapeutic drug release [3].

There are several biological requirements that must be met for a successful tissue engineered device. Specifically for bone tissue, the device should *(i)* be biocompatible, *(ii)* be osteoconductive, which, from a physical view point, requires a porous network, *(iii)* be osteoinductive to attract progenitor cells in order to aid in regeneration, *(iv)* be osteogenic to ensure osteoid deposition, and ultimately *(v)* be osteointegrative. Additionally, material characteristics that should be considered include surface roughness, mechanical integrity, and porosity [3]. Many polymeric materials, both natural and synthetic, have been studied for use as bone scaffolding substrates, including collagen, hyaluronic acid, chitosan, poly(l-lactide-co-glycolide)(PLGA), polymethylmethacrylate (PMMA), polycaprolactone (PCL), as well as several ceramic materials such as calcium phosphate, calcium sulfate and bioactive glass [5–16]. However, the search for a perfect bone scaffold that fulfills all biological criteria still continues. In addition to biological factors, an ideal bone tissue scaffold should also satisfy several physical requirements. For instance, a mismatch between the biomechanics of the orthopedic biomaterial and the native tissue is can also be a source of failure [17]. Often in literature, the biomaterial scaffolding is too compliant to simulate native bone. For example, direct implementation of collagen for bone tissue engineering has been limited due to the relatively weak mechanical characteristics with respect to the native bone [18,19], in spite of the vast amount of interest in this major protein component of native osteoid. Scaffolds made of collagen based-demineralized bone matrix (DBM) reportedly had a wet compressive modulus of 4.1 kPa [20]. This value increased to 31 kPa by crosslinking the DBM with heparin. Despite the significant improvement in rigidity, these values are still too low as compared with the native bone tissue that can have a compressive modulus between 100 to 500 GPa [21].

To improve the mechanical properties and osteoinductive potential of bone scaffold materials, the use of composites has been explored. In many cases, a polymer matrix is augmented by the inclusion of a ceramic material such as hydroxyapatite (HAP), tricalcium phosphate, or bioactive glass [16,22–25]. For example, by synthesizing PLGA microspheres in the presence of amorphous calcium phosphate followed by sintering the spheres produced a porous scaffold with interconnected structures with mechanical properties within the range of the trabecular bone in the dry state [22]. However, the dependence of the mechanical properties of these materials in the hydrated state has not been reported. In another study, dispersing nano-hydroxyapatite (nHAP) throughout silicone rubber provided a more favorable matrix for murine pre-osteoblasts as compared to the pure silicone rubber in terms of cell attachment, viability, and proliferation [23]. In these cases, a polymer matrix was mixed with ceramic filler. This is in contrast to the present study where we reinforce a silk fibroin matrix with a silk fibroin microparticle filler to create a protein-protein composite. By being able to control the interfacial bond between the two phases, we can improve the mechanical performance through interfacial stability.

Bombyx mori (silkworm) silk fibroin is a potent alternative to many other biodegradable biopolymers for bone tissue engineering, due to several desirable properties of this structural protein. Silk fibroin possesses a combination of favorable physical characteristics, such as stiffness and toughness values superior to most natural and synthetic polymers due to its β-sheet (crystalline)-rich structure. For example, individual fibroin filaments have an ultimate tensile strength (UTS) between 610–690 MPa and a modulus between 15 to 17 GPa. In contrast, the UTS for rat tail type I collagen and polylactic acid (PLA) range between 0.9 to 7.4 MPa and 28 to 50 MPa, respectively. The moduli for these materials are 0.0018 to 0.046 GPa, for collagen, and 1.2 to 3.0 GPa for PLA [26]. In addition, silk fibroin has favorable biological characteristics, such as excellent biocompatibility with low inflammatory and immunogenic response. As a consequence, silk has been used as a suture material for centuries and is an FDA approved biomaterial. Moreover, due to its amphiphilic nature, silk fibroin can easily be processed into fibers, hydrogels, thin films, sponges, and composite materials, with degradation rates that can be tuned from days to years [27]. Additionally, silk can be produced in large quantities and at reasonable costs due to the commodity textile business. Due to the above properties and the ability to be processed into a range of material formats, silk is an excellent candidate material for bone tissue applications.

The goal of the present work was to improve the mechanical strength and stiffness of silk fibroin porous sponges while maintaining or improving *in vitro* cell ingrowth and remodeling. Previously, no increase in either material strength or stiffness was observed after depositing hydroxyapatite (HAP) on the surface of preformed silk scaffolds, despite enhanced bone-specific development [28]. Recently, we have shown that silk sponges can be reinforced by loading the matrix phase with different concentrations of silk microparticles in order to address these earlier limitations [29]. Here, we intend to exploit the impressive mechanical properties of these silk-silk composite materials. By adding silk microparticles to the matrix of a silk sponge, both the surface roughness and mechanical properties can be enhanced to address the material specifications required for bone applications. Furthermore, by using a salt leaching technique, a highly porous scaffold can be formed. In this work, silk-silk composites were cultured with human mesenchymal stem cell (hMSC) to observe the possible effects of scaffold stiffness on *in vitro* osteogenic potential. Overall, combined gene expression, biochemical analysis, and μCT imaging data indicate that matrix stiffening significantly increased *in vitro* osteogenic differentiation in 3D porous matrices.

2 Experimental

2.1 Materials

Silk fibroin was extracted from *B. mori* cocoons utilizing the method of Nazarov et al. [30]. Briefly, the sericin protein was removed by boiling the silkworm cocoons in a 0.02 M Na_2CO_3 (Sigma Aldrich, St. Louis, MO) solution for 30 minutes. The resulting fibers were then dissolved in 9.3 M LiBr (Sigma Aldrich, St. Louis, MO) for 4 hours at 60oC and then subsequently dialyzed (MWCO 3,500 Da, Pierce, Rockford, IL) against ultrapure water for 48 hours to remove residual LiBr. Any impurities were removed via centrifugation. The aqueous silk solutions were lyophilized and redissolved in 1,1,1,3,3,3-hexafluoro-2-propanol (HFIP, Sigma Aldrich, St. Louis, MO) to yield a 16 w/v% solution. Scaffolds were generated though porogen salt leaching where 3.4 g of granular NaCl (500 – 600 μm, Fisher Scientific, Fair Lawn, NJ) was used per 1 ml of 16 w/v% silk solution. Reinforcement of the scaffolds was achieved by physically mixing 5 μm diameter silk fibroin particles (see [31] for details on silk microparticle preparation) into the salt prior to adding the silk solution [29,32]. HFIP was allowed to evaporate overnight leading to silk solidification. Afterwards, the dried scaffolds were immersed in methanol for at least one day to induce β-sheet secondary structure. The salt crystals were subsequently extracted by immersion of scaffolds in excess water over two days. The water was changed frequently to ensure complete salt removal. Three different scaffold

types were formed: non-reinforced scaffolds from 16 w/v% silk/HFIP solution (denoted as 1:0), reinforced scaffolds with a 1:1 mass ratio of silk in solution to silk microparticles (1 ml of 16 w/v% silk yields 0.16 g of silk in solution to which 0.16 g of silk microparticles were added), and reinforced scaffolds with a 1:2 ratio by mass of silk in solution to silk microparticles (0.16 g of silk in solution and 0.32 g of silk microparticles).

2.2 Mechanical Testing

A systematic investigation of the compressive modulus and compressive strength of scaffolds with varying particle loading was carried out on an Instron 3366 (Norwood, MA) frame equipped with a 10N capacity. In order to take into account the effects of sample cutting, scaffolds with the same dimensions as those used in the *in vitro* study were examined. Briefly, cylinder-shaped samples measuring 4 mm in diameter and 3 mm in height were prepared prior to testing and only samples with flat surfaces were selected as test specimens. Samples were left hydrated, then set on the bottom platen where a crosshead was lowered until a .01 N load was registered, at which point the sample height was recorded. Tests were conducted at room temperature, under unconfined conditions, in a 0.1 M PBS bath. A displacement control mode was used, with a crosshead displacement rate of 5 mm/min. The compressive modulus was calculated from the slope of the initial linear portion of the compression test and the compressive strength was calculated using a 0.5% offset yield.

The equilibrium Young's modulus of the scaffolds was also measured in unconfined compression in the hydrated state. An initial tare load of 2 grams was applied for 600 seconds. Then a subsequent stress-relaxation test was applied where the specimens were compressed to 10% strain of the scaffold thickness at a ramp velocity of 1% per second and maintained at that position for 1800 seconds. The Young's modulus was obtained from the equilibrium forces measured at 10% strain.

2.3 Cell Culture

All reagents were purchased from Invitrogen (Carlsbad, CA) unless otherwise noted. Human mesenchymal stem cells (hMSCs) were isolated from bone marrow aspirate (Lonza, Gaithersburg, MD) following a modification of the methods of Altman et al. [33]. Briefly, bone marrow aspirate was diluted in Dulbecco's phosphate-buffered saline (DPBS) and cultured for 10 days at 37°C in 5% CO_2. Expansion medium (Dulbecco's modified Eagle medium supplemented with 10% fetal bovine serum, 100 U/ml penicillin, 100 μg/ml streptomycin, 0.25 μg/ml amphotericin, 0.1 mM non-essential amino acids, and 1 ng/ml basic fibroblast growth factor) was added twice a week but spent medium was not removed until cells reached 50% confluence. Once the cells reached above 50% confluence, non-adherent hematopoietic cells were removed via PBS washes and the hMSCs were cultured in expansion medium until either passaged or frozen.

Silk scaffolds 3 mm in height and 4 mm in diameter were prepared and sterilized by autoclaving. After sterilization, sponges were incubated overnight in expansion medium and then aspirated dry prior to hMSC seeding. Cells were inoculated at 1.5×10^6 cells per scaffold. Cultures were incubated in 2.5 ml of osteogenic medium and subsequently maintained by replacing 1.5 ml of medium every 2–3 days. The scaffolds were collected after 3 and 6 weeks. Osteogenic medium consisted of alpha-minimum essential medium (αMEM) supplemented with 10% fetal bovine serum, 100 U/ml penicillin, 100 μg/ml streptomycin, 0.25 μg/ml amphotericin, 0.1 mM non-essential amino acids, 10 mM β-glycerol-2-phosphate (Sigma), 100 nM dexamethasone (Sigma), 0.05 mM L-ascorbic acid (Sigma), and 100 ng/ml human recombinant BMP-2 (Wyeth, Cambridge, MA).

2.4 RT-PCR

RNA isolation and real time reverse transcription polymerase chain reactions (RT-PCR) were carried out using the following protocols. Briefly, cultured scaffolds were stored in Trizol (Invitrogen) and RNA was extracted as per the manufacture's protocol. The aqueous phase was transferred to an RNeasy mini spin column (Qiagen, Valencia, CA), eluted, and then the RNA samples were reverse transcribed into cDNA according the manufacture's protocol (High Capacity cDNA Archive Kit, Applied Biosystems, Foster City, CA). The expression of human collagen type I (COLI), bone sialoprotein (BSP), osteopontin (OP), and alkaline phosphatase (ALP) were quantified using an ABI Prism 7000 real time PCR system (Applied Biosystems) and were normalized against the housekeeping gene, glyceraldehyde-3-phosphate-dehydrogenase (GAPDH). A list of these genes with their abbreviations is shown in Table 1. Primer sequences were purchased from Applied Biosytems (Assay-on-demand) and were detected using a fluorescent TaqMan probe (Invitrogen).

2.5 Biochemical Assays

Scaffolds cultured for 3 and 6 weeks were analyzed for alkaline phosphatase (ALP) activity, calcium and collagen type I accumulation, and DNA content. Assays for DNA and ALP activity were run concurrently by mincing the scaffold in a buffer of 0.2% Triton X-100 (Sigma) with 5 mM magnesium (Sigma). ALP activity was measured using an ALP LiquiColor® kit (Stanbio, Boerne, TX) as per manufacturer's protocol. The sample and reagents were incubated in a 96-well plate for one hour at 37°C and then read at an absorbance of 450 nm. DNA was quantified via a PicoGreen® assay (Invitrogen) and detected on a fluorescent plate reader by exciting at 480 nm and measuring the emission at 528 nm. For calcium analysis, scaffolds were collected in a solution of 5% trichloroacetic acid and minced prior to assay. The accumulated calcium was measured using a total calcium LiquidColor® kit (Stanbio) as per the manufacturer's protocol and read at an absorbance of 550 nm. Type I collagen was determined as previously reported [34]. Briefly, soluble collagen was dissolved by mincing samples in a solution of 1 mg/ml pepsin in 0.5N hydrochloric acid. Films of the solubilized collagen were dried on a 96-well plate and then subsequently incubated in a solution of 1 mg/ml of Direct Red (Sigma) for one hour. Stained samples were fixed with a solution of picric acid, para-formaldehyde, and glacial acetic acid for 10 minutes, rinsed three times with 0.01N HCl, resolubilized in 0.1 N NaOH, and read at an absorbance of 550 nm. All of the biochemical data were normalized to DNA quantity.

2.6 Histology

Formalin-fixed scaffolds were paraffin-embedded at the Histology Laboratory Research Service at Tufts New England Medical Center and subsequent sectioning and staining was performed at the Department of Pathology at Kyunghee University, Seoul, South Korea. Sections were stained for hematoxylin and eosin and von Kossa for calcium. Slides were imaged on a Leica DM IL (Wetzlar, Germany) optical microscope equipped with a 5 megapixel camera.

2.7 MicroCT

μCT was performed using a protocol described in detail in Liu et al [35]. The following settings were used: voltage 55 kV, current 0.109 mA, slice thickness 21 μm, and inter-slice spacing 22 μm. After fixation with formalin, the samples were aligned along their axial direction and stabilized in 1.5 mL micro centrifuge tube. The tube was clamped in the specimen holder of a vivaCT 40 system (SCANCO Medical AG, Basserdorf, Switzerland). The 4-mm length of the scaffold was scanned at 21 μm isotropic resolution. The bone volume was obtained using selected threshold of 220 to binarize gray-scale μCT based on previous thresholding technique [36]. The bone volume fraction (BVF) was calculated by dividing the bone volume by the

volume of the sample. Spatial resolution of this full-voxel model was considered sufficient for evaluating the micro-architecture of the samples, based on the previously established methods [35].

2.8 Statistical Analysis

Statistical analysis was carried out using GraphPad InStat (GraphPad Software, Inc., San Diego, CA). Significance between groups was determined using a Student-Newman-Keuls multiple comparisons test and p-values of less than 0.05 were considered significant.

3 Results

3.1 Mechanical Properties

Table 2 shows that a mass ratio of 1:1 silk in solution to silk microparticles increases the compressive modulus of the scaffolds from 0.28 ± 0.13 MPa for the non-reinforced scaffold to 1.03 ± 0.45 MPa for the silk microparticle reinforced scaffolds. When the ratio of silk microparticles was doubled, an approximate doubling of the compressive modulus was observed when compared to the 1:1 scaffold. For scaffolds with a ratio of 1:2, the hydrated compressive modulus of the scaffold was 1.93 ± 0.88 MPa. Although these stiffness values are higher than those reported for other biopolymer scaffolds [20], they still fall short when compared with that of trabecular bone for which, depending on the location and age of the bone, the elastic modulus can vary between 100 to 500 MPa [21]. Additionally, the equilibrium modulus scaled similarly from 67.19 ± 36.12 kPa to 320.95 ± 145.09 kPa and 981.43 ± 311.92 kPa, for the 1:0, 1:1, and 1:2 scaffolds, respectively. The overall increase in composite stiffness with increasing silk microparticle loading is in agreement with previous reports [29]. We believe that by increasing the particle weight content in the scaffolds, the effective wall thickness increased, which in turn, increased the resistance against pore wall buckling. Published modeling studies [29,37] indicate that such local architectural modifications may lead to a global increase in scaffold modulus as compared with the stiffness of a classical foam. A more thorough analysis of these scaffolds has been carried out and has been published separately [32].

3.2 Molecular Phenotype

Collagen type I gene expression was relatively stable with significant differences only at 6 weeks between the 1:2 reinforced scaffolds and both the non-reinforced control and the 1:1 reinforced scaffolds (Figure 1). Both alkaline phosphatase and osteopontin showed similar trends and were low for all groups except for the highly reinforced, 1:2 scaffolds after 6 weeks in culture. Bone sialoprotein transcript levels were low at the 3 week time point but after 6 weeks there was significant up-regulation for both 1:1 and 1:2 reinforced scaffolds when compared to the non-reinforced scaffolds. Additionally, the up-regulation in the 1:2 reinforced scaffold was significantly higher than that in the 1:1 reinforced scaffolds. Overall, the data indicate that microparticulate reinforcement of silk fibroin scaffold materials increased osteogenic differentiation potential of hMSCs based on bone marker transcript levels.

3.3 Biochemical Analysis

Figure 2 shows the ALP, collagen, and calcium deposition for non-reinforced controls and 1:1 and 1:2 reinforced composite scaffolds. Both ALP activity and collagen content were relatively stable between all scaffold types and time points, with an insignificant increase in values from week 3 to week 6 for ALP. In contrast with the ALP results, calcium deposition increased significantly from none at week 3 for all the scaffold types (insignificant cross-sample difference in calcium deposition values) to 0.6, 0.7, and 1.3 mg/μg of DNA after 6 weeks of culture for non-reinforced, 1:1, and 1:2 reinforced scaffolds, respectively.

3.4 Histology

Histological analysis indicated that the cells penetrated the scaffolds (Figure 3A–B). Cells were dense at the surface of the constructs and with some cells within the center of the scaffolds (approximately 1.5 mm). We believe that there were fewer cells in the center regions most likely due to the static culture conditions. Von Kossa staining (Figure 3A) showed limited calcification after 3 weeks in culture on the reinforced scaffolds and no calcium on the non-reinforced control. After 6 weeks, all the scaffolds showed mineralization (Figure 3B). In the non-reinforced scaffold, the mineralization was predominantly pericellular, with few nucleation sites starting within the silk matrix. In contrast, for both 1:1 and 1:2 reinforced scaffolds, calcification was evident within the silk composite scaffold. Control experiments without cells did not show any calcification, indicating that the mineralization is due to cellular deposition.

3.5 MicroCT

Scaffold calcification was also confirmed via μCT imaging. Analysis of the scaffolds after 3 weeks of incubation indicated no mineralization (data not shown), commensurate with histology staining and biochemical assays. After 6 weeks in culture, bone volume fractions for non-reinforced, 1:1, and 1:2 reinforced scaffolds were 0.008, 0.071, and 0.067, respectively (Figure 4). Mineral formation was advanced for both 1:1 and 1:2 reinforced scaffolds with respect to the non-reinforced control scaffold and had the appearance of trabecular-like structures found in bone.

Discussion

Previous work in our lab focused on post-processing mineralization of porous silk scaffolds utilizing calcium chloride and sodium phosphate [28]. This attempt was successful in building up hydroxyapatite within the pores of the scaffold, which in turn stimulated the cells toward osteogenesis, albeit with no significant improvement in scaffold mechanical properties due to mineral deposition. In addition, increased rounds of mineralization may also reduce pore sizes and therefore reduce the ability of the cells to penetrate into the scaffolds. In this paper, we used an alternative strategy, specifically with silk microparticle reinforcement, for the improvement of the mechanical properties of porous silk sponges without the risk of reducing the pore size. Through this work, it was found that silk microparticle reinforcement, presumably through increasing the compressive modulus of silk scaffolds, increased the ability of hMSCs to differentiate along the osteogenic lineage as evidenced by cellular mineral deposition.

In the present study, 5 μm silk particles were incorporated into the silk matrix during processing to create a protein-protein composite. The ability to optimize the interfacial contact between the matrix and filler phases is critical to maximize the mechanical properties of a composite [38]. If the reinforcing agent has superior mechanical properties but the interface between the filler and the matrix is weak, the composite will fail along the interface. Therefore, strong interfacial binding is essential to facilitate transfer of the mechanical load from the matrix to the reinforcing agent and vice versa. In the present study, silk microparticles were incorporated into the silk matrix, specifically during solution processing. The inclusion of particles at a 1:2 ratio with the silk in solution increased the hydrated compressive modulus up to 1.93 ± 0.88 MPa, to approach that of trabecular bone (100 to 500 MPa [21]). These results suggest that an effective load transfer was achieved between the silk fibroin sponge matrix and the silk fibroin microparticle reinforcement, presumably through a strong interfacial contact that was possible through solution processing. As the amount of reinforcing particles was increased, the scaffolds became stiffer and therefore closer to the modulus of trabecular bone. Ultimately, the mechanical properties of the scaffolding may be an important consideration for potential *in vivo* applications. This work evaluates the use of an entirely protein-based composite system

with a better match of mechanical properties to that of the native tissue as compared to other protein-based systems, for example collagen. However, the compressive modulus of silk composite scaffolds is still significantly lower than that of native tissue. Therefore, we would expect potential application of these materials as temporary, biodegradable conduits for bone regeneration. The expected gradual degradation of the silk scaffold may allow for the concomitant replacement of the scaffold with the regenerated tissue. It is at this stage that we hope to achieve improved tissue regeneration through improved scaffold mechanical properties as compared to other protein scaffolds.

We observed that the hMSCs differentiated into osteoblasts with an increased rate of differentiation on more rigid scaffolds. Osteoblastic differentiation occurs in several phases [19]. Initially, osteoid, consisting of type I collagen, fibronectin, and other growth factors, is deposited by osteoblasts. As the cells mature, collagen continues to be secreted as well as ALP and matrix gla protein. Eventually, collagen secretion slows down and osteocalcin and osteopontin are produced to aid in mineralization. Transcript levels for OP, ALP, and COL1 all show the highest levels for the highly reinforced (1:2) scaffold at 6 weeks, with the exception of BSP which was significantly higher for both the 1:1 and 1:2 scaffolds at 6 weeks as compared with the non-reinforced control. Since BSP is known to bind to calcium [19], these data correspond with the μCT data where there was a significant difference between the non-reinforced and both reinforced scaffolds.

Protein levels showed consistent ALP activity for all scaffold types at both 3 weeks and 6 weeks. Meinel et al. previously demonstrated that ALP had a biphasic pattern over time in culture [19]. Since only 3 and 6 weeks were assessed in the current study, it was difficult to determine a possible change in the ALP activity. Additionally, there was no significant difference in collagen accumulation among different scaffolds, although collagen levels increased over time for all scaffolds. This may indicate a leveling off on collagen secretion and an increase in mineralization, particularly since calcium levels increased and the μCT and histology images showed enhanced mineralization on all the scaffolds. The exact mechanism by which calcium was localized within the silk scaffolds at 6 weeks is not clear and will warrant further research.

It is not surprising that increasing the rigidity of the scaffold enhanced the differentiation of hMSCs into osteoblasts as defined by mineral deposition. Mechanical forces are known to be vital for wound healing and tissue homeostasis in adult organisms [39]. Matrix stiffening may increase cellular contractibility and matrix deposition. In addition, the role of matrix stiffness in cell motility and behavior has also been explored [40] and shown to influence differentiation. Particularly, hMSCs differentiate into an osteogenic lineage on stiffer substrates whereas the cells appeared more neurogenic on more compliant matrices [41]. Previous work from our lab gave similar results in a 3-D environment where softer matrices influenced hMSCs towards a chondrogenic lineage [42]. We were able to generate more mature osteogenic cells on silk fibroin composites with stiffer compressive moduli. The mechanics of these materials approach native bone. It is believed that cells detect the rigidity of these materials which in turn may drive them towards an osteogenic lineage. In addition, the possible role of surface roughness cannot be ruled out and is the focus of ongoing work. Other future work will explore animal models to extend the *in vitro* observations reported here to bone healing *in vivo*.

Conclusions

There is a major clinical need for versatile, slowly degrading, biomaterial systems for bone repair that also mimic the architecture and mechanical functions of native bone. We report the formation of a protein-protein composite through the use of silk fibroin microparticle reinforcements to increase the compressive properties of porous silk fibroin sponges. These

materials better mimicked the mechanical features of native bone and significantly increased the osteogenic differentiation potential of hMSCs. Future work will address *in vivo* integration and utility of these matrices for bone repair.

Acknowledgments

The authors would like to thank Professor Heinz Redl from the Ludwig Boltzmann Institute for the hBMP-2, Reynald Lescarbeau for isolating the hMSCs, and Dr. Tuna Yucel for his help with revising this manuscript. This work has been funded by NIH grant number P41 EB002520 for the Tissue Engineering Resource Center.

References

1. Drosse I, Volkmer E, Capanna R, Biase PD, Mutschler W, Schieker M. Tissue engineering for bone defect healing: An update on a multi-component approach. Injury 2008;39:S9. [PubMed: 18804579]
2. Marquis M-E, Lord E, Bergeron E, Drevelle O, Park H, Cabana F, Senta H, Faucheux N. Bone cells-biomaterials interactions. Frontiers in Bioscience 2009;14:1023. [PubMed: 19273115]
3. Khan Y, Yaszemski MJ, Mikos AG, Laurencin CT. Tissue Engineering of Bone: Material and Matrix Considerations. Journal of Bone and Joint Surgery - American Volume 2008;90:36.
4. Holy, CE.; Volenec, FJ.; Geesin, J.; Bruder, SP. Bone Regeneration. In: Lanza, R.; Langer, R.; Vacanti, J., editors. Principles of Tissue Engineering. Amsterdam, Boston, Heidelberg, London, New York, Oxford, Paris, San Diego, San Francisco, Singapore, Sydney, Tokyo: Academic Press; 2007. p. 845
5. Barralet J, Gbureck U, Habibovic P, Vorndran E, Gerard C, Doillon CJ. Angiogenesis in Calcium Phosphate Scaffolds by Inorganic Copper Ion Release. Tissue Engineering Part A 2009;15:1601. [PubMed: 19182977]
6. Borden M, Attawia M, Khan Y, Laurencin CT. Tissue engineered microsphere-based matrices for bone repair: design and evaluation. Biomaterials 2002;23:551. [PubMed: 11761175]
7. Jiang T, Abdel-Fattah WI, Laurencin CT. In vitro evaluation of chitosan/poly(lactic acid-glycolic acid) sintered microsphere scaffolds for bone tissue engineering. Biomaterials 2006;27:4894. [PubMed: 16762408]
8. Laurencin CT, Ambrosio AMA, Borden MD, Cooper JA. Tissue Engineering: Orthopedic Applications. Annual Review of Biomedical Engineering 1999;1:19.
9. Oh SH, Park IK, Kim JM, Lee JH. In vitro and in vivo characteristics of PCL scaffolds with pore size gradient fabricated by a centrifugation method. Biomaterials 2007;28:1664. [PubMed: 17196648]
10. Shimko DA, Nauman EA. Development and characterization of a porous poly(methyl methacrylate) scaffold with controllable modulus and permeability. Journal of Biomedical Materials Research Part B-Applied Biomaterials 2007;80B:360.
11. Song H-Y, Esfakur Rahman AHM, Lee B-T. Fabrication of calcium phosphate-calcium sulfate injectable bone substitute using chitosan and citric acid. J Mater Sci Mater Med 2009;20:935. [PubMed: 19052849]
12. Tay BKB, Patel VV, Bradford DS. Calcium sulfate- and calcium phosphate-based bone substitutes - Mimicry of the mineral phase of bone. Orthopedic Clinics of North America 1999;30:615. [PubMed: 10471766]
13. Vogelin E, Jones NF, Huang JI, HBJ, Lieberman JR. Healing of a critical-sized defect in the rat femur with use of a vascularized periosteal flap, a biodegradable matrix, and bone morphogenic protein. Journal of Bone and Joint Surgery - American Volume 2005;87-A:1323.
14. Uemura T, Dong J, Wang Y, Kojima H, Saito T, Iejima D, Kikuchi M, Tanaka J, Tateishi T. Transplantation of cultured bone cells using combinations of scaffolds and culture techniques. Biomaterials 2003;24:2277. [PubMed: 12699664]
15. Livingston T, Ducheyne P, Garino J. In vivo evaluation of a bioactive scaffold for bone tissue engineering. Journal of Biomedical Materials Research 2002;62:1. [PubMed: 12124781]
16. Zhang K, Ma Y, Francis LF. Porous polymer/bioactive glass composites for soft-to-hard tissue interfaces. Journal of Biomedical Materials Research 2002;61:551. [PubMed: 12115445]

17. Thelen S, Barthelat F, Brinson LC. Mechanics considerations for microporous titanium as an orthopedic implant material. Journal of Biomedical Materials Research Part A 2004;69A:601. [PubMed: 15162401]

18. Ambrose WM, Salahuddin A, So S, Ng SY, Marquez SP, Takezawa T, Schein O, Elisseeff J. Collagen Vitrigel Membranes for the In Vitro Reconstruction of Separate Corneal Epithelial, Stromal, and Endothelial Cell Layers. Journal of Biomedical Materials Research Part B-Applied Biomaterials 2009;90B:818.

19. Meinel L, Fajardo R, Hofmann S, Langer R, Chen J, Snyder B, Vunjak-Novakovic G, Kaplan D. Silk implants for the healing of critical size bone defects. Bone 2005;37:688. [PubMed: 16140599]

20. Lin H, Zhaol Y, Sun WJ, Chen B, Zhang J, Zhao WX, Xiao ZF, Dai JW. The effect of crosslinking heparin to demineralized bone matrix on mechanical strength and specific binding to human bone morphogenetic protein-2. Biomaterials 2008;29:1189. [PubMed: 18083224]

21. Rezwan K, Chen QZ, Blaker JJ, Boccaccini AR. Biodegradable and bioactive porous polymer/inorganic composite scaffolds for bone tissue engineering. Biomaterials 2006;27:3413. [PubMed: 16504284]

22. Khan YM, Katti DS, Laurencin CT. Novel polymer-synthesized ceramic composite-based system for bone repair: An in vitro evaluation. Journal of Biomedical Materials Research Part A 2004;69A:728. [PubMed: 15162415]

23. Thein-Han WW, Shah J, Misra RDK. Superior in vitro biological response and mechanical properties of an implantable nanostructured biomaterial: Nanohydroxyapatite-silicone rubber composite. Acta Biomaterialia 2009;5:2668. [PubMed: 19435616]

24. Wei GB, Ma PX. Structure and properties of nano-hydroxyapatite/polymer composite scaffolds for bone tissue engineering. Biomaterials 2004;25:4749. [PubMed: 15120521]

25. Zhang Y, Wu C, Friis T, Xiao Y. The osteogenic properties of CaP/silk composite scaffolds. Biomaterials. In Press, Corrected Proof.

26. Altman GH, Diaz F, Jakuba C, Calabro T, Horan RL, Chen J, Lu H, Richmond J, Kaplan DL. Silk-based biomaterials. Biomaterials 2003;24:401. [PubMed: 12423595]

27. Vepari C, Kaplan DL. Silk as a biomaterial. Progress in Polymer Science 2007;32:991. [PubMed: 19543442]

28. Kim HJ, Kim UJ, Kim HS, Li CM, Wada M, Leisk GG, Kaplan DL. Bone tissue engineering with premineralized silk scaffolds. Bone 2008;42:1226. [PubMed: 18387349]

29. Rajkhowa R, Gil ES, Kluge J, Numata K, Wang L, Wang X, Kaplan DL. Reinforcing Silk Scaffolds with Silk Particles. Macromolecular Bioscience 2010;10:599. [PubMed: 20166230]

30. Nazarov R, Jin HJ, Kaplan DL. Porous 3-D scaffolds from regenerated silk fibroin. Biomacromolecules 2004;5:718. [PubMed: 15132652]

31. Rajkhowa R, Wang LJ, Wang XG. Ultra-fine silk powder preparation through rotary and ball milling. Powder Technology 2008;185:87.

32. Gil ES, Kluge JA, Rockwood DN, Rajkhowa R, Wang L, Wang X, Vunjak-Novakovic G, Kaplan DL. Mechanical Improvements to Reinforced Porous Silk Scaffolds. Macromolecular Biosci. In press.

33. Altman GH, Horan RL, Martin I, Farhadi J, Stark PRH, Volloch V, Richmond JC, Vunjak-Novakovic G, Kaplan DL. Cell differentiation by mechanical stress. FASEB J 2001:01.

34. Park S-H, Ji Hao C, So Ra P, Byoung-Hyun M. Potential of Fortified Fibrin/Hyaluronic Acid Composite Gel as a Cell Delivery Vehicle for Chondrocytes. Artificial Organs 2009;33:439. [PubMed: 19473139]

35. Liu XS, Sajda P, Saha PK, Wehrli FW, Guo XE. Quantification of the Roles of Trabecular Microarchitecture and Trabecular Type in Determining the Elastic Modulus of Human Trabecular Bone. Journal of Bone and Mineral Research 2006;21:1608. [PubMed: 16995816]

36. Grayson WL, Bhumiratana S, Grace Chao PH, Hung CT, Vunjak-Novakovic G. Spatial regulation of human mesenchymal stem cell differentiation in engineered osteochondral constructs: effects of pre-differentiation, soluble factors and medium perfusion. Osteoarthritis and Cartilage. In Press, Corrected Proof.

37. Gibson LJ. Biomechanics of cellular solids. Journal of Biomechanics 2005;38:377. [PubMed: 15652536]

38. Desai AV, Haque MA. Mechanics of the interface for carbon nanotube-polymer composites. Thin-Walled Structures 2005;43:1787.

39. Legant WR, Pathak A, Yang MT, Deshpande VS, McMeeking RM, Chen CS. Microfabricated tissue gauges to measure and manipulate forces from 3D microtissues. Proceedings of the National Academy of Sciences of the United States of America 2009;106:10097. [PubMed: 19541627]

40. Discher DE, Janmey P, Wang YL. Tissue cells feel and respond to the stiffness of their substrate. Science 2005;310:1139. [PubMed: 16293750]

41. Engler AJ, Sen S, Sweeney HL, Discher DE. Matrix elasticity directs stem cell lineage specification. Cell 2006;126:677. [PubMed: 16923388]

42. Ghosh S, Laha M, Mondal S, Sengupta S, Kaplan DL. In vitro model of mesenchymal condensation during chondrogenic development. Biomaterials 2009;30:6530. [PubMed: 19732950]

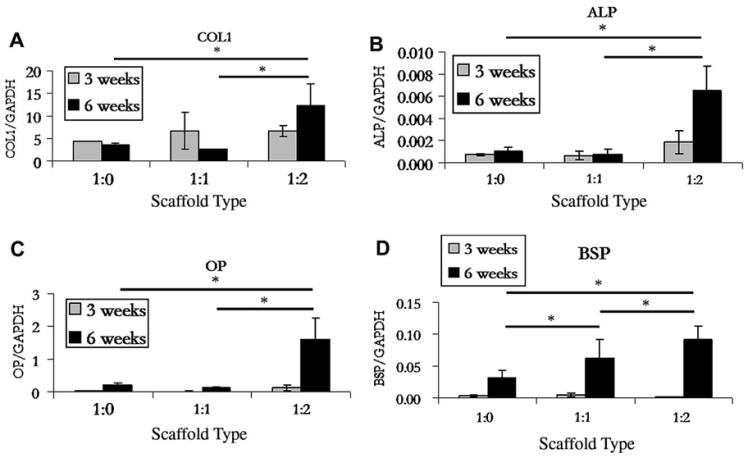

Figure 1.

RT-PCR analysis of transcript levels for osteogenic differentiation markers collagen type I (COL1), alkaline phosphatase (ALP), bone sialoprotein (BSP), and osteopontin (OP). Significant differences are indicated by an asterisk ($p<0.05$). Data shown are mean ± S.D., n = 3.

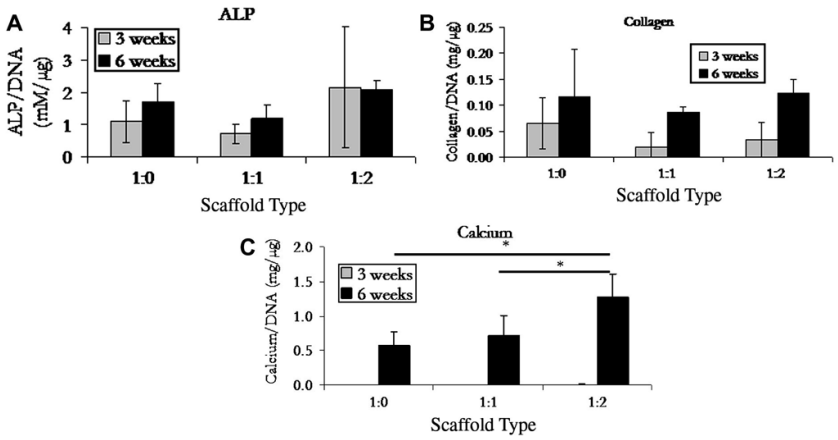

Figure 2.

Biochemical analysis of alkaline phosphatase, soluble collagen, and calcium levels monitored at 3 and 6 week. Data shown as mean ± S.D., n=3, significant difference is denoted with an asterisk ($p<0.05$). There was no significant difference found between all samples in both the ALP and collagen assays.

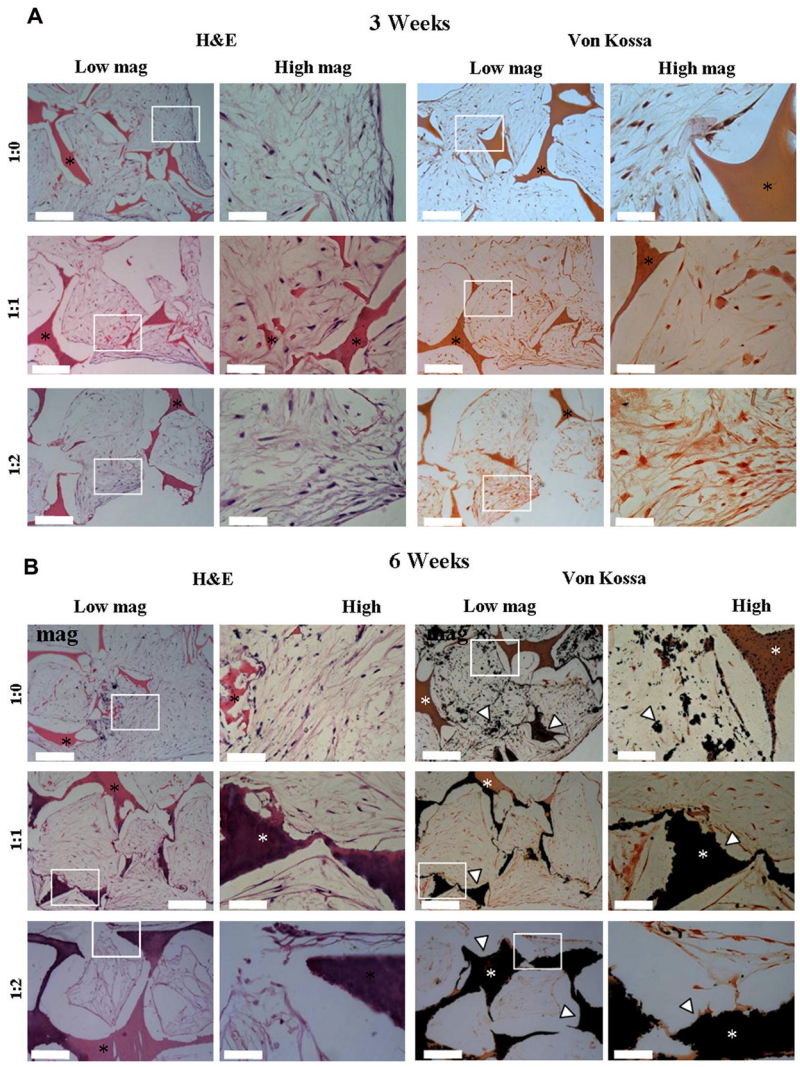

Figure 3.

A–B. Histology of scaffolds after (A) 3 and (B) 6 weeks. Left panel: H&E and right panel: von Kossa. The asterisk denotes the silk scaffold and the light arrow head indicates calcium. Scale bars equal 200 μm (low magnification) and 50 μm (high magnification).

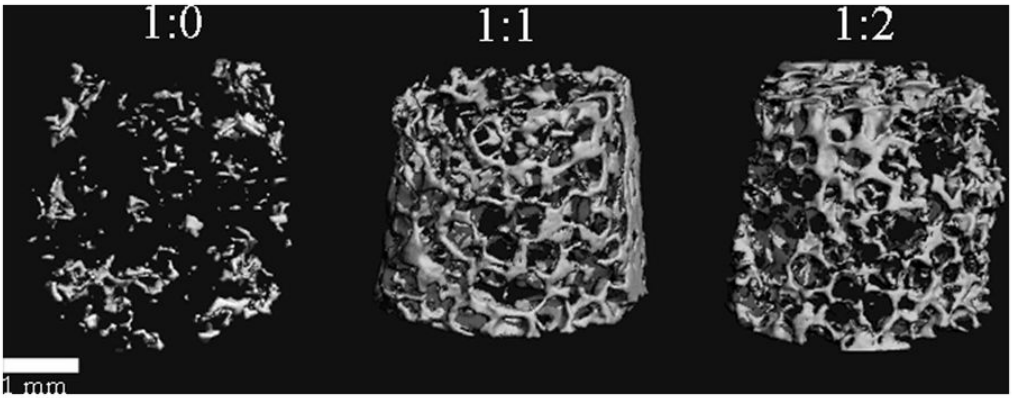

Figure 4.
MicroCT analysis of mineral deposition at 6 weeks. Analysis of the scaffolds after 3 weeks of incubation indicated no mineralization (commensurate with histology staining and biochemical assays) and therefore is not shown. After 6 weeks in culture, the bone volume fraction for 1:0, 1:1, and 1:2 was 0.0077, 0.0709, and 0.0667, respectively. Mineral formation for both of the reinforced scaffolds was advanced with respect to the nonreinforced control scaffold and had the appearance of trabecular bone. Scale bar equals 1 mm.

Table 1

Genes probed by RT-PCR and their abbreviations.

Gene	Abbreviation
Glyceraldehyde-3-phosphate-dehydrogenase	GAPDH
Collagen type I	COL1
Bone sialoprotein	BSP
Osteopontin	OP
Alkaline phosphatase	ALP

Table 2

Hydrated mechanical properties of reinforced silk scaffolds under compressive force. Data shown are mean ± S.D., n = 4.

Silk sponges	Compressive modulus	Yield stress	Equilibrium Modulus
1:0	0.28 ± 0.13 MPa	22.6 ± 6.3 kPa	67.19 ± 36.13 kPa
1:1	1.03 ± 0.45 Mpa	50.4 ± 28.6 kPa	320.95 ± 145.09 kPa
1:2	1.93 ± 0.88 Mpa	154.9 ± 77.5 kPa	981.43 ± 311.92 kPa